Bivariate Grid-Connection Speed Control of Hydraulic Wind Turbines

Chao Ai, Wei Gao, Lijuan Chen, Jiawei Guo, Xiangdong Kong, Andrew Plummer

***Abstract*—The requirement for a grid-connected wind turbine is that the synchronous generator speed is stable within a required speed range for the power grid. In this paper, a hydraulic wind turbine (HWT) system ~~(HWT)~~ is considered, and the working principle and working conditions of the HWT are introduced. A novel speed control method is proposed in this paper, using both a proportional flow control valve and a variable displacement motor, which are adjusted in combination to control the speed of the HWT. By establishing a state space model of the HWT and solving the nonlinear system with a feedback linearization method, a bivariate tracking controller is constructed to realize accurate speed control under fluctuating wind speed and the load disturbance conditions. The effectiveness of the control method is verified by simulation, but experimental results highlight problems with the method. Based on these results, the theoretical control law is simplified to reduce sensitivity to measurement noise and modelling error, and the effectiveness of the control law is finally verified experimentally. It lays a theoretical foundation for the practical application of HWT.**

***Index Terms*—**Synchronous grid-connection; Hydraulic power take off; Feedback linearization; Hydrostatic transmission

I INTODUCTION

Wind energy is a vast renewable energy resource being increasingly tapped by wind turbines which are growing in number and size. Conventional wind turbine~~s~~ transmissions consist of a mechanical gearbox and high speed generator, or sometimes direct drive low-speed generators are used as described in [1]. But these two traditional transmission schemes have some disadvantages, such as high cost and high failure rate. In order to reduce the cost and improve the reliability, hydrostatic transmissions have been proposed in [2-4]. Thus the power captured by the turbine rotor will be transmitted to the generator through the hydrostatic transmission, and the generator can be flexibly installed, either in the nacelle of the wind turbine, or installed on the ground driven via hydraulic pipelines, which greatly reduces the difficulty of installation and maintenance. The b~~B~~enefits of the hydraulic wind turbine (HWT) are that the hydrostatic transmission is inherently more compliant than the mechanical transmission, which makes it more reliable in the face of shock loading, and the transmission ratio is adjustable, so the system does not need additional frequency conversion devices to coordinate wind turbine speed and power grid frequency. Meanwhile, with the development of digital hydraulic technology, the low part-load efficiencies of conventional hydraulics is solved[5].

As a new type of wind power generation technology, the HWT has been the subject of several research and development studies[6-10]. Grid connection is one of the key requirements for wind power generation. Thus the HWT needs to control the generator speed to be stable in grid frequency if a cost-effective synchronous generator is to be used, even though the wind speed and generator load are varying. Various methods have been proposed to satisfy the above need. An energy storage system is introduced in the HWT, and two control loops regulating the accumulator pressure and hydraulic motor speed are proposed to keep the motor speed constant in [11], but ~~an~~ experimental verification is not carried out. A variable displacement hydraulic motor and flow control valve are used to realize the grid connection speed control of the HWT in [12], but the flow control valve in the control structure is located between the high pressure and low pressure lines. This allows a bypass flow which is used for speed control, but also causes a flow loss and hence power loss. An accumulator is used to smooth the fluctuations of the hydraulic system and realize the speed control in [13], and

This work is supported in part by the National Natural Science Foundation of China under Grant 51775476, in part by the Excellent Youth Project of Hebei ,China under Grant E2018203388. (*Corresponding author: ~~Xiangdong Kong , and Plummer Andrew~~Chao Ai.*)

C. Ai, W. Gao, W. Guo, and X. Kong are with School of mechanical engineering, Yanshan University, Qinhuangdao 066004, China (e-mail:aichao@ysu.edu.cn;gaowei2018@njit.edu.cn; 708951592@stumail.ysu.edu.cn; xdkong@ysu.edu.cn). A Plummer is with the Department of Mechanical Engineering, University of Bath, Bath BA2 7~~3~~AY, UK (email: A.R.Plummer@bath.ac.uk); L. Chen is with the Nanjing Institute of Technology, Nanjing 211167, China (e-mail: chenlj@njit.edu.cn).

Formatted: Not Superscript/ Subscript

Formatted: Not Superscript/ Subscript

the pressure of the high-pressure line can be stabilized, but when the rotor speed is too high, the system will still lose flow through a relief valve. A compensation control method for speed reduction based on the pressure feedback is put forward in [14], and ~~the~~ high-precision motor speed control is realized. However, the control of the motor speed is not considered with random changes of pump speed and hence flow. The speed of the motor is compensated by detecting the rotor speed, and using a fuzzy control method to give good dynamic characteristics in [15], but the system always adjusts to connect to the grid smoothly under the wind speed disturbance. An adaptive fuzzy sliding-mode control (AFSMC) is proposed for the speed control of a hydraulic pressure coupling drive in [16]. To handle changes of wind speed and load power, a double-loop speed control scheme is proposed to hold the motor speed at the synchronous speed in [17]. However, there is no explanation of relevant experiments. For a HWT with a fixed displacement pump and a fixed displacement motor as the hydraulic main transmission system, under wind and load disturbances, a proportional flow control valve is used to control the flow rate between the main and auxiliary generators to control the main generator speed in [18]. However there is only one control variable, and the control accuracy is relatively poor.

In view of the relevant literature on speed control of HWTs connected to the grid, a better control accuracy method is still required, which considers the various disturbance factors while ensuring that the system maximizes power capture. Therefore, this paper introduces a proportional flow control valve in the original hydraulic transmission system, that is, the valve is added between the hydraulic fixed displacement pump and the hydraulic variable displacement motor. And a feedback linearization method is adopted to realize coordinated control of the valve and the motor displacement (swash plate angle). This method is required to achieve quasi-synchronous grid-connected control of the HWT, in the presence of random disturbances at the wind turbine input and the motor load output.

The contents of this paper are organized as follows. Section II describes the composition of HWT as well as section III presents the corresponding mathematical models. Section IV shows the proposed controller design process, which consists of bivariate control based on the feedback linearization. Section V presents the experimental results plus the corresponding analysis. Some conclusions are given in Section VI. Through the research of this paper, the practical popularization of the HWT is planned to be realized.

II DESCRIPTION OF THE HWT

The hydraulic wind turbine is composed of a rotor, a fixed displacement hydraulic pump, a variable displacement hydraulic motor and a synchronous generator. An inverter for frequency conversion is not required. The rotor and the pump are coaxially connected, and the pump supplies high pressure oil to the motor, so the fluctuation of the wind speed tends to affect the motor speed [19-20]. The motor and the generator are also coaxially connected, and changing the motor displacement can control the motor and generator speed. When the synchronous generator is stable within the required speed range for the grid, it can be connected to the grid for power generation. A schematic diagram of the HWT is shown in Fig.1.

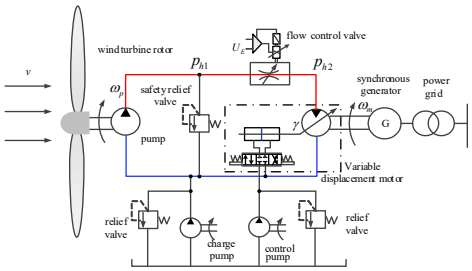

Fig.1. Schematic of the HWT

In order to satisfy the power quality requirements, the synchronous generator frequency should be consistent with the power grid, e.g. in China, the national power grid frequency is 50 ±0.2 Hz, which gives a required 1500 ± 6 r/min to the generator and hydraulic motor.

To achieve this target, the control method described in this paper aims to improve the performance of the main transmission system of HWT. A proportional flow control valve is added between the pump and the motor, which gives a degree of isolation from the influence of the wind speed fluctuation on the motor speed.

Before the HWT is connected to the grid, the output torque of the motor is close to zero, and the rotor is allowed to accelerate freely due to the low load pressure. The load change of the synchronous generator is abrupt when the grid is connected, so it is difficult to control the motor speed ~~stable~~ to be within the required speed range.

Commented [AP1]: ??? do you mean "but the system does not always adjust to connect to…"

The control method introduced in this paper uses feedback linearization to realize the linear correspondence between the desired output and the control input, and indirectly controls the rotor speed, which makes the system flow relatively stable. The motor inlet pressure is controlled by the motor displacement, and the motor speed is kept stable under the sudden change of the synchronous generator load. By controlling the flow control valve voltage signal and the motor swash plate angle, the system is intended to achieve precise speed control at any wind speed, and the system can be smoothly connected to the grid under all conditions.

III THE MATHEMATICAL MODEL OF THE HWT

3.1 Rotor aerodynamic model

The power captured and aerodynamic torque developed by the turbine rotor are given by [21]:

$$P_r = \frac{1}{2}\rho\pi R^2 v^3 C_p(\lambda,\beta) \tag{1}$$

$$T_r = \frac{P_r}{\omega_r} \tag{2}$$

where, P_r is the wind power captured by the rotor. ρ is the air density. R is the rotor radius. v is the effective average wind speed. $C_p(\lambda,\beta)$ is the wind energy utilization coefficient. λ is the tip speed ratio, $\lambda=R\omega_r/v$. β is the pitch angle. T_r is the rotor aerodynamic torque, and ω_r is the rotor speed.

The wind energy utilization coefficient is given by [22]:

$$C_p(\lambda,\beta)=C_1\left(\frac{C_2}{\lambda_i}-C_3\beta-C_4\right)e^{-\frac{C_5}{\lambda_i}}+C_6\lambda \tag{3}$$

$$\frac{1}{\lambda_i}=\frac{1}{\lambda+0.08\beta}+\frac{0.0035}{\beta^3+1} \tag{4}$$

where, C_1, C_2, C_3, C_4, and C_5 are the rotor parameters which are determined by manufacturing data.

Because the rotor is coaxially connected to the pump, i.e. $\omega_r=\omega_p$, thus

$$T_r=\frac{P_r}{\omega_r}=\frac{1}{2\omega_p}\rho\pi R^2 v^3 C_p\left(\lambda,\beta\right)=T_v\left(\omega_p,v\right) \tag{5}$$

where, ω_p is the pump speed, and $T_v(\omega_p,v)$ characterizes the rotor torque as a function of pump speed.

3.2 Hydraulic transmission system model

The pump shaft torque is related to the pressure developed by:

$$T_p=\frac{D_p p_{h1}}{\eta_{mech,p}} \tag{6}$$

where, D_p is the hydraulic pump displacement. p_{h1} is the pressure difference between the pump suction and discharge lines. $\eta_{mech,p}$ is the pump mechanical efficiency, which is assumed to be unity.

The difference between the rotor and pump torque accelerates their combined inertia, and overcomes viscous friction:

$$T_v\left(\omega_p,v\right)-T_p=J_p\frac{\mathrm{d}\omega_p}{\mathrm{d}t}+B_p\omega_p \tag{7}$$

where, J_p is the moment of inertia of the rotor and pump, and B_p is the pump damping coefficient.

Pump volume flow rate and speed are related by:

$$Q_p=D_p\omega_p-C_{t1}p_{h1} \tag{8}$$

where, Q_p is the pump flow rate, and C_{t1} is the pump leakage coefficient.

From the equations (6)-(8), the state equation of the hydraulic pump speed can be expressed as

$$\dot{\omega}_p=\frac{1}{J_p}\left(T_r-\frac{D_p p_{h1}}{\eta_{mech,p}}-B_p\omega_p\right) \tag{9}$$

Similarly, the motor output torque is related to pressure by:

$$T_m=D_m p_{h2}\eta_{mech,m}=K_m\gamma p_{h2}\eta_{mech,m} \tag{10}$$

where, T_m is the torque generated by the motor. D_m is the motor displacement, $D_m=K_m\gamma$. p_{h2} is the pressure difference between motor inlet and outlet. $\eta_{mech,m}$ is the mechanical efficiency of the motor, which is assumed to be unity. K_m is the motor maximum displacement. γ is non-dimensional displacement fraction, ranging from 0 to 1.

The difference between the motor and generator torque accelerates the motor inertia, and overcomes the viscous friction:

$$T_m-T_L=J_m\frac{\mathrm{d}\omega_m}{\mathrm{d}t}+B_m\omega_m \tag{11}$$

where, T_L is the motor load torque. J_m is the moment of inertia of the motor. ω_m is the motor speed. B_m is the motor damping coefficient.

And the motor volume flow rate and speed are related by:

$$Q_m=D_m\omega_m+C_{t2}p_{h2} \tag{12}$$

where, Q_m is the motor flow rate, and C_{t2} is the motor leakage coefficient.

From the equations (10)-(12), the state equation of the

motor speed is:

$$\dot{\omega}_m = \frac{1}{J_m}\left(K_m\gamma p_{h2}\eta_{mech,m} - B_m\omega_m - T_L\right) \tag{13}$$

The flow through the proportional flow control valve is:

$$Q_{bl} = KU_E \tag{14}$$

where, K is the proportional coefficient, and U_E is the voltage signal.

The oil flows between pump and motor inside a hose, and the general equation for the additional flow caused by oil compressibility and hose compliance is:

$$Q_c = \frac{V}{\beta_e}\frac{\mathrm{d}p_h}{\mathrm{d}t} \tag{15}$$

where, Q_c is the flow rate caused by the oil compression. V is the pressure-affected oil volume. β_e is the effective oil bulk modulus including a correction for hose expansion. p_h is the oil pressure in the high pressure line hose.

The proportional flow control valve divides the high pressure line into two parts, one is the pump to the flow control valve, with volume V_1, and the other part is the flow control valve to the motor, with volume V_2.

The compressibility flow between the pump and the flow control valve is given by:

$$Q_{c1} = Q_p - Q_{bl} = D_p\omega_p - C_{t1}p_{h1} - KU_E \tag{16}$$

The compressibility flow between the flow control valve and the motor is:

$$Q_{c2} = Q_{bl} - Q_m = KU_E - D_m\omega_m - C_{t2}p_{h2} \tag{17}$$

To establish the state space model of the main transmission system for the HWT, the following assumptions need to be made:

(1) The pressure in the low pressure line is held constant by the charge pump and its associated relief valve.

(2) The leakage coefficient, the viscous damping coefficient and the bulk modulus of the oil are the fixed values, which do not change with temperature or other factors.

(3) The pressure loss in the hydraulic lines is ignored.

The system state space model without grid connection dynamics is obtained, through combining the equations (9), (13)-(17).

$$\begin{cases} \dot{\omega}_p = \dfrac{D_p}{J_p}\omega_p - \dfrac{D_p}{J_p}p_{h1} + \dfrac{1}{J_p}T_v\left(\omega_p, v\right) \\ \dot{p}_{h1} = \dfrac{D_p\beta}{V_1}\omega_p - \dfrac{C_{t1}\beta}{V_1}p_{h1} - \dfrac{K\beta U_E}{V_1} \\ \dot{p}_{h2} = \dfrac{K\beta U_E}{V_2} - \dfrac{C_{t2}\beta}{V_2}p_{h2} - \dfrac{K_m\beta\omega_m}{V_2}\gamma \\ \dot{\omega}_m = \dfrac{K_m p_{h2}}{J_m}\gamma - \dfrac{1}{J_m}T_L \end{cases} \tag{18}$$

The state variables and control inputs are selected as follows: $x_1 = \omega_p$, $x_2 = p_{h1}$, $x_3 = p_{h2}$, $x_4 = \omega_m$, $u_1 = U_E$, and $u_2 = \gamma$.

So the system state space model can also be expressed as:

$$\begin{cases} \dot{x}_1 = \dfrac{D_p}{J_p}x_1 - \dfrac{D_p}{J_p}x_2 + \dfrac{1}{J_p}T_v\left(x_1, v\right) \\ \dot{x}_2 = \dfrac{D_p\beta_e}{V_1}x_1 - \dfrac{C_{t1}\beta_e}{V_1}x_2 - \dfrac{K\beta_e}{V_1}u_1 \\ \dot{x}_3 = \dfrac{K\beta_e}{V_2}u_1 - \dfrac{C_{t2}\beta_e}{V_2}x_3 - \dfrac{K_m\beta_e}{V_2}x_4u_2 \\ \dot{x}_4 = \dfrac{K_m}{J_m}x_3u_2 + \dfrac{1}{J_m}T_L \end{cases} \tag{19}$$

The system is organized into affine nonlinear form $\dot{\boldsymbol{x}} = \boldsymbol{f}(\boldsymbol{x}) + \boldsymbol{g}(\boldsymbol{x})\boldsymbol{u}$, where

$$\boldsymbol{f}(\boldsymbol{x}) = \begin{cases} -\dfrac{B_p}{J_p}x_1 - \dfrac{D_p}{J_p}x_2 + \dfrac{1}{J_p}T_v\left(x_1, v\right) \\ \dfrac{D_p\beta_e}{V_1}x_1 - \dfrac{C_{t1}\beta_e}{V_1}x_2 \\ -\dfrac{C_{t2}\beta_e}{V_2}x_3 \\ -\dfrac{B_{\mathrm{m}}}{J_{\mathrm{m}}}x_3 - \dfrac{1}{J_{\mathrm{m}}}T_{\mathrm{L}} \end{cases} \tag{20}$$

and the two columns of $\boldsymbol{g}(\boldsymbol{x})$ are:

$$\begin{aligned} \boldsymbol{g}_1(\boldsymbol{x}) &= \begin{bmatrix} 0 & -\dfrac{K\beta_e}{V_1} & \dfrac{K\beta_e}{V_2} & 0 \end{bmatrix}^{\mathrm{T}} \\ \boldsymbol{g}_2(\boldsymbol{x}) &= \begin{bmatrix} 0 & 0 & -\dfrac{K_m\beta_e x_4}{V_2} & \dfrac{K_m x_3}{J_m} \end{bmatrix}^{\mathrm{T}} \end{aligned} \tag{21}$$

IV THE BIVARIATE CONTROL BASED ON FEEDBACK LINEARIZATION

4.1 Determination of the system output

In order to realize the control scheme, the output power of the pump and the motor inlet pressure are selected as the outputs. Thus

$$y = \begin{cases} h_1(x) = D_p\omega_p p_{h1} = D_p x_1 x_2 \\ h_2(x) = p_{h2} = x_3 \end{cases} \tag{22}$$

4.2 The relative order of the system

From the equations (20) and (21), according the relevant definition of the Lie derivative [22], the relative order is:

$$\begin{aligned} L_{g_1} L_f^0 h_1(\boldsymbol{x}) &= -K\frac{\beta_e}{V_1} D_p x_1 \\ L_{g_2} L_f^0 h_2(\boldsymbol{x}) &= -\frac{K_m \beta_e \omega_m}{V_2} \end{aligned} \tag{23}$$

This gives the relative order of the system as $\sigma=\{1,1\}$, that is, the relative order $\sigma<4$, thus the system cannot be completely linearized. Therefore, input - output linearization and the zero dynamic design method are adopted to determine the controller for the system [23].

In the process of zero dynamic design, the system dynamic behavior can be divided into the external dynamics and internal dynamics. The external dynamics are not only required to be stable but also have tracking performance and reject disturbance. The internal dynamics are only required to be stable.

4.3 Zero dynamic controller design

The two zero dynamics selected in this paper are $\eta_3(x)=x_1$ and $\eta_4(x)=x_4$, the pump speed and the motor speed respectively, which are considered as the internal dynamics. First, a coordinate transformation of the system gives

$$\begin{cases} z_1 = \varphi_1(x) = h_1(x) = D_p x_1 x_2 \\ z_2 = \varphi_2(x) = h_2(x) = x_3 \\ z_3 = \eta_3(x) = x_1 \\ z_4 = \eta_4(x) = x_4 \end{cases} \tag{24}$$

Therefore, the Jacobian matrix of the vector function $\boldsymbol{\phi}(\boldsymbol{x})=[z_1(\boldsymbol{x}) \quad z_2(\boldsymbol{x}) \quad z_3(\boldsymbol{x}) \quad z_4(\boldsymbol{x})]^{\mathrm{T}}$ at $\boldsymbol{x}=\boldsymbol{x}_0$ is:

$$\frac{\partial \boldsymbol{\phi}}{\partial \boldsymbol{x}} = \begin{bmatrix} \frac{\partial \varphi_1}{\partial x_1} & \frac{\partial \varphi_2}{\partial x_1} & \frac{\partial \varphi_3}{\partial x_1} & \frac{\partial \eta_1}{\partial x_1} \\ \frac{\partial \varphi_1}{\partial x_2} & \frac{\partial \varphi_2}{\partial x_2} & \frac{\partial \varphi_3}{\partial x_2} & \frac{\partial \eta_2}{\partial x_2} \\ \frac{\partial \varphi_1}{\partial x_3} & \frac{\partial \varphi_2}{\partial x_3} & \frac{\partial \varphi_3}{\partial x_3} & \frac{\partial \eta_3}{\partial x_3} \\ \frac{\partial \varphi_1}{\partial x_4} & \frac{\partial \varphi_2}{\partial x_4} & \frac{\partial \varphi_3}{\partial x_4} & \frac{\partial \eta_4}{\partial x_4} \end{bmatrix}^{\mathrm{T}} = \begin{bmatrix} D_p x_2 & D_p x_1 & 0 & 0 \\ 0 & 0 & 1 & 0 \\ 1 & 0 & 0 & 0 \\ 0 & 0 & 0 & 1 \end{bmatrix}^{\mathrm{T}} \tag{25}$$

This is a non-singular at $\boldsymbol{x}=\boldsymbol{x}_0$, so the coordinate transformation is valid.

And then the inverse mapping of $\boldsymbol{z}=\boldsymbol{\phi}(\boldsymbol{x})$ is $\boldsymbol{x}=\boldsymbol{\phi}^{-1}(\boldsymbol{z})$. Therefore, the $\boldsymbol{x}$ can be expressed as a function of $\boldsymbol{z}$, as follows:

$$\begin{cases} x_1 = z_3 \\ x_2 = \dfrac{z_1}{D_p z_3} \\ x_3 = z_2 \\ x_4 = z_4 \end{cases} \tag{26}$$

The final expression of the system in $\boldsymbol{z}$ coordinates can be obtained from the equations (19) and (26).

$$\begin{cases} \dot{z}_1 = D_p z_3 \left(-\dfrac{B_p}{J_p} z_3 - \dfrac{D_p}{J_p} \dfrac{z_1}{D_p z_3} + \dfrac{1}{J_p} T_v(z_3, v) \right) \\ \quad + D_p z_3 \left(\dfrac{D_p \beta_e}{V_1} z_3 - \dfrac{C_{t1} \beta_e}{V_1} \dfrac{z_1}{D_p z_3} \right) - \dfrac{K \beta_e D_p z_3}{V_1} u_1 \\ \dot{z}_2 = u_1 - \dfrac{C_{t2} \beta_e}{V_2} z_2 - \dfrac{K_m \beta_e}{V_2} z_4 u_2 \\ \dot{z}_3 = \dfrac{D_p}{J_p} z_3 - \dfrac{D_p}{J_p} \dfrac{z_1}{D_p z_3} + \dfrac{1}{J_p} T_v(z_3, v) \\ \dot{z}_4 = \dfrac{K_m z_2}{J_m} u_2 - \dfrac{1}{J_m} T_L \end{cases} \tag{27}$$

The system output in the $\boldsymbol{z}$ coordinate system is:

$$y = \begin{cases} D_p \omega_p p_{h1} = D_p x_1 x_2 = z_1 \\ p_{h2} = x_3 = z_2 \end{cases} \tag{28}$$

The external states, which are the pump outlet power and motor inlet pressure, are close to zero and in a stable state, that is, $z_1 = z_2 = 0$, $\dot{z}_1 = \dot{z}_2 = 0$. At this point, the equation (27) can be expressed as:

$$\begin{cases} \dot{z}_3 = \dfrac{D_p}{J_p} z_3 + \dfrac{1}{J_p} T_v(z_3, v) \\ \dot{z}_4 = \dfrac{K_m z_2}{J_m} u_2 - \dfrac{1}{J_m} T_L \end{cases} \tag{28}$$

That is, when the external states are close to zero, the internal state stability is related to the external load of the pump and motor, and it is irrelevant to u_1 and u_2, but all are asymptotically stable. Therefore, the system has zero dynamic stability and can be solved by the controller[24].

After the coordinate transformation and the zero dynamic design of the system, the feedback controller can be designed. The specific method is to linearize the system in the coordinate system and construct a pseudo-linear system. Under the pseudo-linear system, the output and the control input of the system are linearly related.

First, the desired control input is constructed as $\dot{z}_3 = f_1$ and $\dot{z}_4 = f_2$. At this point, the output of the system and the two artificially constructed inputs f_1 and f_2, are linearly

dependent. The constructed input are as follows:

$$\begin{cases} f_1 = D_p x_2 \left(-\frac{B_p}{J_p} x_1 - \frac{D_p}{J_p} x_2 + \frac{1}{J_p} T_v\left(x_1, v\right) \right) \\ \quad + D_p x_1 \left(\frac{D_p \beta}{V_1} x_1 - \frac{C_{t1}\beta}{V_1} x_2 \right) - \frac{K\beta D_p x_1}{V_1} u_1 \\ f_2 = \frac{K\beta}{V_2} u_1 - \frac{C_{t2}\beta}{V_2} x_3 - \frac{K_m \beta}{V_2} x_4 u_2 \end{cases} \tag{29}$$

Thus, the valve and motor control inputs can be expressed in terms of f_1 and f_2:

$$\begin{cases} u_1 = \frac{V_1}{K\beta D_p x_1} \left[\begin{array}{l} D_p x_2 \left(-\frac{B_p}{J_p} x_1 - \frac{D_p}{J_p} x_2 + \frac{1}{J_p} T_v\left(x_1, v\right) \right) \\ + D_p x_1 \left(\frac{D_p \beta}{V_1} x_1 - \frac{C_{t1}\beta}{V_1} x_2 \right) - f_1 \end{array} \right] \\ u_2 = \frac{K u_1 - C_{t2} x_3 - \frac{V_2}{\beta} f_2}{K_m x_4} \end{cases} \tag{30}$$

4.4 Output reference design

At this point, the system output and the inputs f_1 and f_2 are already linearly dependent. It is necessary to find the relationship between the pump output power and motor inlet pressure and pump speed and motor speed, so as to achieve the purpose of controlling the rotor speed and motor speed.

The pump output power is intended to be controlled so that the pump (and rotor) can reach the optimal rotational speed at any wind speed. The system is expected to carry out tracking control, and the reference value is set as:

$$y_{1d} = K_P \omega_p^3 = K_P x_1^3 \tag{31}$$

where, K_P is power coefficient.

The motor inlet pressure is controlled to ensure the motor speed is stable at 1500 r/min. The specific method is to construct the kinetic energy function of the motor, and the referenced pressure is determined by the stability of a Lyapunov energy function.

The kinetic energy of the motor is:

$$E = \frac{1}{2} J_m \omega_m^2 \tag{32}$$

where, E is the motor kinetic energy.

The Lyapunov energy function is:

$$\dot{} \quad \cdot \quad \nu_m^{\ 2} + p_{h2} D_m \omega_m - T_L \omega_m \tag{33}$$

and the desired value of the motor inlet pressure is:

$$y_{2d} = p_{h2d} = \frac{B_m \omega_{md} + T_L}{D_m} \tag{34}$$

where, ω_{md} is the required motor speed, and p_{h2d} is the desired value of the motor inlet pressure.

When the desired value of the inlet pressure is y_{2d}, the control system has the following characteristics. If the hydraulic motor speed satisfies the inequation of $\omega_m < \omega_{md}$, the motor inlet pressure will satisfy the inequation of $p_{h2} > \frac{B_m \omega_m + T_L}{D_m}$, that is, $\dot{}$, the motor accelerates. When the hydraulic motor speed reaches the required power-frequency speed, the motor inlet pressure will satisfy the function $p_{h2} = \frac{B_m \omega_m + T_L}{D_m}$, the motor stops to accelerate, and the motor speed is stable within the required speed range. Similarly**,** if the motor speed satisfies the inequation of $\omega_m > \omega_{md}$, the motor inlet pressure will satisfy the inequation $p_{h2} < \frac{B_m \omega_m + T_L}{D_m}$, that is, $\dot{}$, and the motor decelerates. Therefore, taking the motor pressure as the control output, the system is asymptotically stable at the required power-frequency speed.

4.5 Controller design

In the control of the grid-connected speed, theoretically, the system is linearized precisely by feedback. However, in reality, there will exist tracking errors due to model parameters. The closed loop PI control is used to reduce the tracking error.

The tracking error is defined as:

$$e = y_{\mathrm{d}} - y \tag{35}$$

And the new control input[25] is:

$$\begin{aligned} f_1 &= \dot{} \quad + k_{12} \int e_1 \mathrm{d}t \\ f_2 &= \dot{} \quad + k_{22} \int e_2 \mathrm{d}t \end{aligned} \tag{36}$$

In equation (36), the values of k_{11}、k_{12}、k_{21} and k_{22} are turned according to the control requirements.

The final controller is given by equations (30) and (35). The controller expressed in terms of physical variables is:

$$\begin{cases} U_E = \frac{D_p \omega_p - C_{t1} p_{h1} + V_1 p_{h1} \dot{} \quad \cdot V_1 f_1 / \beta_e D_p \omega_p}{K} \\ \gamma = \frac{K U_E - C_{t2} p_{h2} - \frac{V_2}{\beta_e} f_2}{K_m \omega_m} \end{cases} \tag{37}$$

According to the equation (37), the system states and constructed control inputs are combined linearly to form the control signal for the flow control valve voltage and

motor displacement. Through the real-time detection of system states, the calculated control signals are sent to the system to realize the grid-connected speed control.

V THE SIMULATION AND EXPERIMENTAL VERIFICATION

5.1 The simulation verification of control law

On the basis of the above controller, the mathematical simulation model is established in Matlab®/Simulink® to verify whether the controller can meet the control requirements.

The coefficients in the utilization factor used in equation (3) are shown in Table 1. The other HWT parameters are shown in Table 2. The simulation model for the turbine, hydraulics and controller is shown in Fig.2.

Table 1 Coefficients of wind energy utilization factor

C_1	C_2	C_3	C_4	C_5	C_6
0.5176	116	0.4	5	21	0.0068

Table 2 Simulation parameters

Symbol	Quantity	Numerical value
P_r	Rated power	24 kW
v	Rated wind speed	13 m/s
R	Rotor radius	3.74 m
$C_{p\max}(\lambda,\beta)$	Maximum utilization coefficient of wind energy	0.4496
$\lambda_{\max}$	Optimum tip speed ratio	22.77
B_p	Pump damping coefficient	0.40 (Nms/rad)
D_p	Pump displacement	1×10^{-5} (m^3/rad)
J_p	Moment of inertia for the wind turbine and the pump	400 (kg/m^3)
K_m	Motor displacement gradient	5.366×10^{-6} (m^3/rad)
B_m	Motor damping coefficient	0.03 (Nms/rad)
J_m	Moment of inertia for the motor	0.46 (kg/m^3)
β_e	Oil volume elastic modulus	743×10^6 Pa
C_t	Leakage coefficient	6.28×10^{12} (m^3/(sPa))
V	High pressure line volume	2.8×10^{-3} m^3

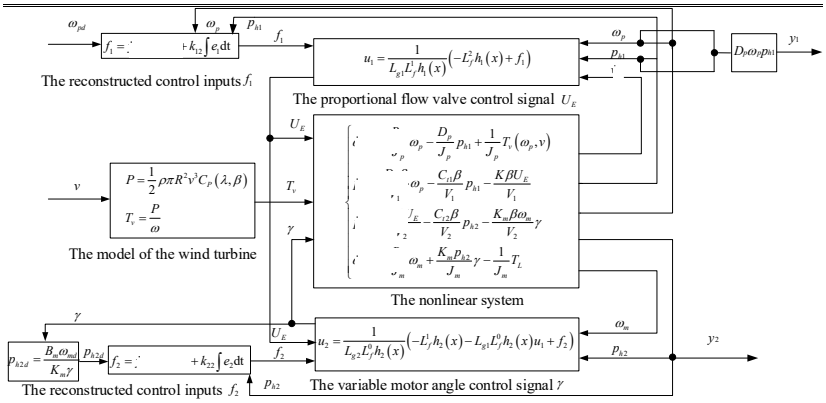

Fig.2 Motor speed controlled simulation model

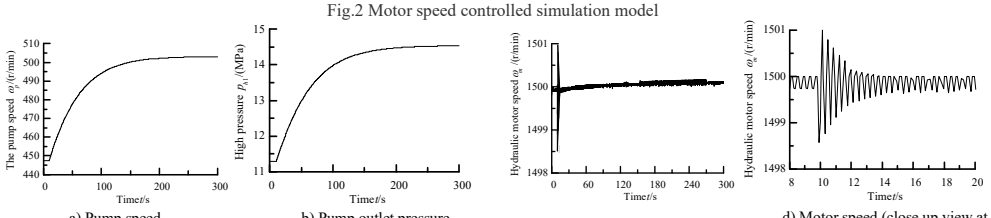

a) Pump speed b) Pump outlet pressure c) Motor speed d) Motor speed (close up view at step time)

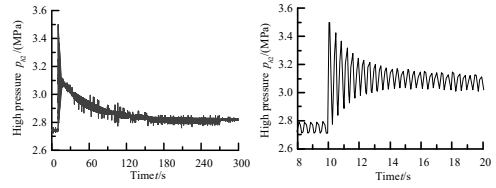

e) Motor inlet high pressure f) Motor inlet high pressure (close up view at step time)

Fig.3. The response characteristics with step change in wind speed at 10s.

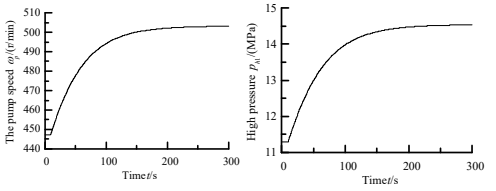

a) Pump speed b) Pump outlet pressure

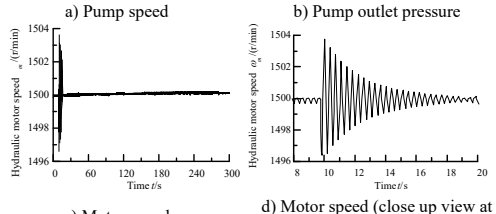

c) Motor speed d) Motor speed (close up view at step time)

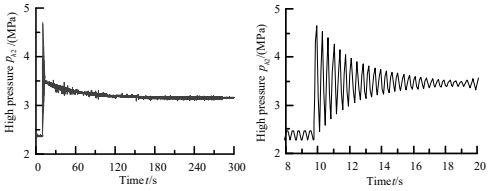

e) Motor inlet high pressure f) Motor inlet high pressure (close up view at step time)

Fig. 4. The response characteristics with a step load disturbance and step change in wind speed at 10s

Under the conditions of no motor load disturbance and a step change in wind speed from 8 m/s to 9 m/s at 10s, each state response is shown in Fig.3. With a step disturbance of the motor load, e.g. from 1Nm to 4Nm, and a step change in wind speed from 8 m/s to 9 m/s at 10s, each state response is shown in Fig.4.

From the results of Figs.3 and 4, when there is only the step change in wind speed without other disturbances, the motor speed is perturbed by ±1 r/min. When the motor load and the wind speed step occur simultaneously, the motor speed is perturbed by ±4 r/min. In the control process, the rotor speed tracks the given value, while the high pressure between the pump and the flow control valve and the high pressure between the proportional flow valve and the hydraulic motor are increased. The flow control valve will consume part of the energy to ensure the system is in a stable state, and the heat produced during the regulation process is discharged by the hydraulic cooling system. Thus it is verified that the control strategy proposed in this paper can ensure the HWT remains synchronized with the grid during a step change in wind speed and motor load.

Under the conditions of 8 ±0.5 m/s in wind speed and a step change of motor load disturbance, e.g. from 1 Nm to 4 Nm, each state response is shown in Fig.5.

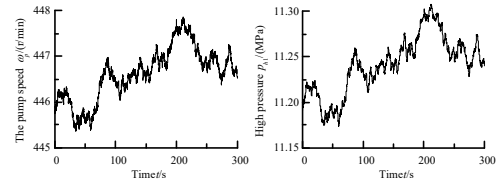

a) Pump speed b) Motor speed

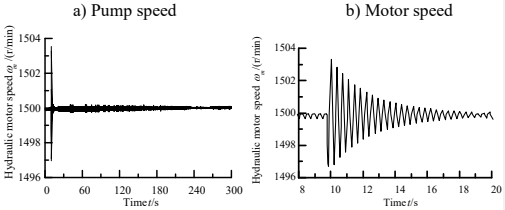

c) Motor speed d) Motor speed (close up view at step time)

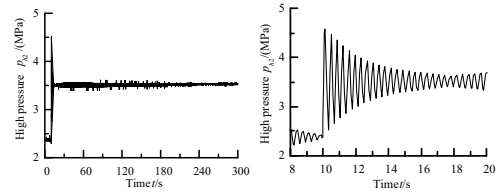

e) Motor inlet pressure f) Motor inlet high (close up view at step time)

Fig.5 The response characteristics with random wind speed and step change in load disturbance at 10s

From the results of Fig.4 and 5, it can be seen that the HWT connects to the grid smoothly under different operating conditions. And after the generator connects to the grid, changing the pressure between the flow control valve and motor, the pressure can track the pressure between the pump and flow control valve. When the pressure of the two high-pressure lines are the same, the flow control valve is at its maximum opening, and the HWT will enter into the maximum power point tracking mode.

5.2 Experimental verification of the control law

In order to verify the control law validity, an experimental study is carried out based on a 24kW HWT

experimental platform, which is shown in Fig.6.

Fig.6 24 kW hydraulic wind turbine experimental platform

Under a step change in pump speed, the experimental curves of the motor speed and pressure are shown in Fig.7 and 8.

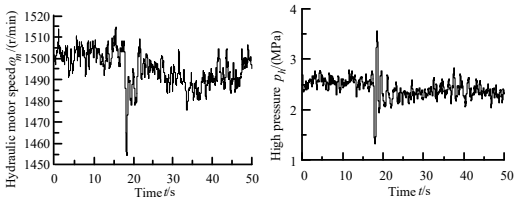

a) Motor speed b) High pressure

Fig. 7 The pump speed at the step of 600 r/min - 700 r/min at 17s

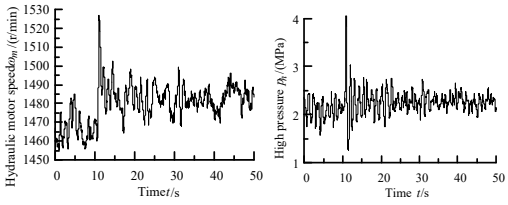

a) Motor speed b) High pressure

Fig. 8 The pump speed at the step of 900 r/min - 800 r/min at 10s

The motor speed is kept close to 1500 r/min, although not within the desired speed range. But the response trend is basically the same as with the simulation, and the system is asymptotically stable.

The main factors leading to the low accuracy of the motor speed control are as follows.

(1)The motor speed control accuracy depends on the torque sensor accuracy and the motor viscous damping coefficient, of which is not a constant due to the motor swing angle and actual rotation speed, plus the torque sensor accuracy is very low at small measurement range.

(2)The motor speed control law contains the leakage coefficient, which is not a constant and closely relates to the system operating condition.

(3)The pressure state is introduced into the motor speed control, which is very sensitive to higher order dynamics.

5.3 Practical control law design

Although there are many difficulties for practical implementation of the theoretical control law, it can provide a design direction. The engineering implementation of the theoretical control law is explored in this section. From the expression (30), the final motor speed control law is

$$u_2 = \frac{1}{L_{g2}L_f^0 h_2(\boldsymbol{x})}\left(-L_f^1 h_2(\boldsymbol{x}) - L_{g1}L_f^0 h_2(\boldsymbol{x})u_1 + f_2\right) = \frac{Ku_1 - C_{t2}p_{h2} - \frac{V_2}{\beta_e}f_2}{K_m\omega_m} \tag{38}$$

Taking the pressure p_{h2} as the output, the desired output is

$$p_{h2d} = \frac{B_m\omega_{md} + T_L}{D_m} \tag{39}$$

And the restructured control input is

$$f_2 = k_{21}e_2 + k_{22}\int e_2 dt \tag{40}$$

In order to solve the deficiencies of the theoretical control law, the control law will be simplified to meet the engineering requirements.

The control law consists of the flow control valve flow, the system leakage flow, and the oil compression flow. The simplification process is carried out in the following three aspects.

(1) The first is the leakage flow caused by the pressure. The experimental results show that the high-pressure line pressure is small before connection to the grid. Thus, if the system pressure value is not introduced in the control, that is, $C_{t2}p_{h2} = C$, the system oscillation can be avoided.

(2) The measured motor speed state is required in equation (38), but it introduces sensor noise. The motor speed control target is a constant, and so the measured speed is replaced by a fixed value to improve the control accuracy.

(3) The third one is the hydraulic oil compression flow rate caused by the change of pressure. The pressure deviation is obtained by the motor torque balance equation, so it is difficult to get the accurate value. Therefore, the accuracy of the control system is very low. In the actual control, the measured pressure deviation is introduced into the controller.

Therefore, the practical simplified control law is

$$u_2 = \frac{Ku_1 - C_{\text{leak}} - \left(k_1 \Delta\omega_p + k_2 \int \Delta\omega_p \mathrm{d}t\right)}{K_m \omega_{md}} \tag{41}$$

The experimental results to validate the simplified control law are shown in Figs.9, 10, 11 and 12. Different step changes in pump speed are given, e.g. from 460 r/min to 480 r/min~~ at 1s~~, 560 r/min to 550 r/min~~ at 2s~~, 800 r/min to 810 r/min ~~at 3s~~ and 810 r/min to 800 r/min~~ at 1s~~, and the corresponding motor speed is measured accordingly.

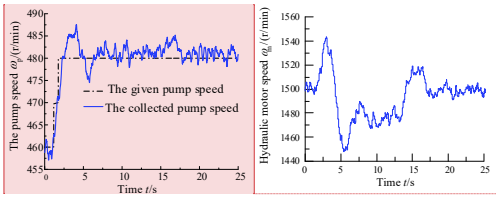

Fig.9 Step change in demand p~~P~~ump speed of 460 r/min - 480 r/min at 1s

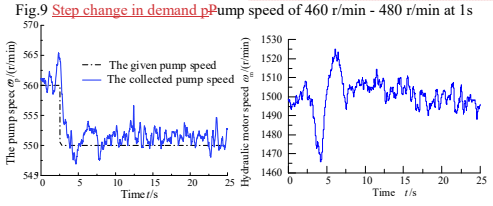

Fig.10 Step change in demand pump~~P~~ump speed of 560 r/min - 550 r/min at 2s

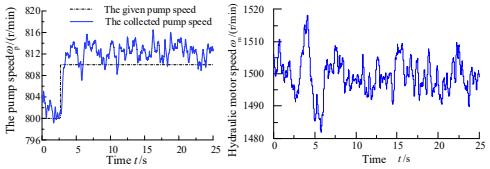

Fig.11 Step change in demand pump~~P~~ump speed of 800 r/min - 810 r/min at 3s

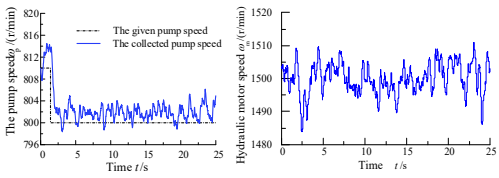

Fig.12 Step change in demand pump~~P~~ump speed of 810 r/min - 800 r/min at 1s

From the comparison between Fig.9 and 11, as well as, Fig.10 and 12, the higher the pump speed is, the smaller the motor speed fluctuation will be. ~~Vice versa for low pump speed.~~ The reason is when the pump is operating at low speed, the system leakage is large, the difference between the constant flow benchmark and the required value is significant, and the system tends to ~~oscillate easily~~be lightly damped.

Comparinge Fig.9 and 10, as well as~~,~~ Fig.11 and 12, with a rising step change in pump speed, the motor speed fluctuation is larger~~, but one is smaller with a decreasing step~~, which is mainly due to the system leakage is not following the changing trend of the flow.

~~Additionally~~To summarise, with different step changes in rotor ~~-~~pump speed, the motor-generator speed is stabilized at the power ~~-~~frequency speed with high precision. ~~In the process of th~~Fore grid connection speed control, ~~-the~~a flow control valve and the proposed control method ~~is used to~~can ensure the ~~output flow~~generator speed is relatively ~~stable~~constant.

VI CONCLUSION

In order to develop the controller for HWTs, a state space model before grid connection is established, and a bivariate control method is proposed, which adjusts a flow control valve and the motor displacement. The flow control valve controls the HWT output power and indirectly controls the motor speed, and the motor swing angle (i.e. displacement) controls the motor inlet pressure. Based on this theoretical control method, experimental results show that the motor speed is stable at 1500 ± 20 r/min with wind speed fluctuation and motor load disturbance, but it does not satisfy the accuracy requirements for the speed control to synchronize with the grid frequency. Thus, the factors affecting the accuracy of control law are analyzed, and combined with practical requirements, and hence the control law is simplified. Finally, using the simplified control law, when the input flow rate changes in a small range, the motor speed is stable at 1500 ± 6 r/min, and

Commented [AP2]: Change 'given' to 'demand' and 'collected' to 'measured' in the legends of these 4 figures

Commented [AP3]: From figures 9-12, this is not true. In fact the transient response looks worse than Fig 7/8, given that the speed change is much bigger (but the steady state accuracy is better). Ideally, you would show the experimental results for the two versions of the controller under the same conditions with the same variables plotted so they can be directly compared.

meanwhile the control method establishes a theoretical basis for the HWT low voltage ride through control. Note that in the results presented here, the generator and motor are lightly loaded, and so to moderate the speed of the rotor and pump there is significant power loss through the flow control valve; this would not be the case with greater generator output and hence motor load. The research provides a very promising control method which enables wider use of HWT's in the future, addressing the reliability issues associated with conventional designs incorporating mechanical gearboxes.

REFERENCE

[1] J. Wei, W. Sun, A. Guo, and L. Wang, "Analysis of wind turbine transmission system considering bearing clearance and thermo-mechanical coupling," in *Proc. World Non-Grid-Connected Wind Power Energy Conf*., Nanjing, China, 2009, pp. 1–5.

[2] Z. G. Liu, G. L. Yang, L. J. Wei and D. L. Yue, "Variable speed and constant frequency control of hydraulic wind turbine with energy storage system," *Adv. Mech. Eng.*, vol. 9, n.8, pp. 1-10, Aug. 2017, 10.1177/1687814017715195.

[3] K. A. Stelson, Saving the world's energy with fluid power, in *Proc. 8th JFPS Int. Symp. Fluid Power*, Okinawa, Japan, 2011, pp. 1–7.

[4] Z. Y. Jiang, L. M. Yang, Z. Gao and T. Moan, "Numerical simulation of a wind turbine with a hydraulic transmission system," *Energy Procedia*, vol.53, pp.44-55, Sept. 2014, 10.1016/j.egypro. 2014.07.214.

[5] N. H. Pedersen, P. Johansen, T. O. Andersen, "Optimal control of a wind turbine with digital fluid power transmission", *Nonlinear Dyn.*, vol. 91, no. 1, pp. 591-607, Nov. 2018, 10.1007/s11071-017-3896-0.

[6] M. L. Cai, Y. X. Wang, Z. X. Jiao and Y. Shi, "Review of fluid and control technology of hydraulic wind turbines," *Front. Mech. Eng.*, vol. 12, no. 3, pp. 312-320, Jan. 2017, 10.1007/s11465-017-0433-2.

[7] A C Mahato, S K Ghoshal, A K Samantaray, "Reduction of wind turbine power fluctuation by using priority flow divider valve in a hydraulic power transmission", *Mech. Mach. Theory*, vol. 128, pp. 234-253, Jun. 2018, https://doi.org/10.1016/j.mechmachtheory. 2018.05. 019.

[8] Wei L, Liu Z, Zhao Y, et al. "Modeling and Control of a 600 kW Closed Hydraulic Wind Turbine with an Energy Storage System," *Appl. Sci.*, vol. 8, no. 8, pp. 1-19, Aug. 2018, 10.3390/app8081314

[9] X. Yin, X. Tong, X. Zhao, et al. "Maximum power generation control of a hybrid wind turbine transmission system based on h∞ loop-shaping approach," *IEEE Trans. Sustain. Energy*, 2019, 10.1109/TSTE.2019.2897549.

[10] C. Ai, W. J. Bai, T. Y. Zhang, et al. "Active control of pressure resonance in long pipeline of bottom founded hydraulic wind turbines based on multi-objective genetic algorithm," *IEEE Access*, vol. 6, pp. 53368-53380, Oct. 2018, 10.1109/ACCESS.2018. 2871462

[11] A. Izadian, S. Hamzehlouia, M. Deldar and S. Anwar, "A hydraulic wind power transfer system: Operation and modeling," *IEEE Trans. Sustain. Energy,* vol. 5, no. 2, pp. 457–465, Mar. 2014, 10.1109/TSTE.2013.2291835.

[12] P. Chapple and M. O. K. Niss, A method and system for connecting a wind turbine system to an electric grid, EUROPE Patent 2481915A1, Aug., 2012.

[13] H. T. Do, T. D. Dang, H. V. A. Truong, et al, "Maximum power point tracking and output power control on pressure coupling wind energy conversion system," *IEEE Trans. Ind. Electron.*, vol. 65, n.2, pp. 1316-1324, Jul. 2018, 10.1109/TIE.2017.2733424.

[14] T. H. PENG, N. G. YUE, "Speed loss compensation experiment study in variable-speed pump-control-motor system". *J. Mech. Eng.*, vol. 48, n. 4, pp. 175-181, Feb. 2012, 10.3901/JME.2012.04.175.

[15] H. Zhang, G. F. Zhang, Z. Q. Xiong and B. Zheng, "Velocity control of hydraulic motor in hydraulic wind turbines," *Liaoning Gongcheng Jishu Daxue Xuebao, Ziran Kexueban*, vol. 31, n. 4, pp. 536-539, Aug. 2012.

[16] T. H. Ho and K. K. Ahn, "Speed control of a hydraulic pressure coupling drive using an adaptive fuzzy sliding-mode control," *IEEE/ASME Trans. Mechatronics*, vol. 17, no. 5, pp. 976-986, Oct. 2012, 10.1109/TMECH.2011.2153866.

[17] L. J. Wei, Z. G. Liu, Y. Y. Zhao, G. Wang and Y. H. Tao, "Modeling and control of a 600 kW closed hydraulic wind turbine with an energy storage system," *Appl. Sci.*, vol. 8, no. 8, pp.1-18, Aug. 2018, 10.3390/app8081314.

[18] Vaezi M, Asgharifard A, Izadian A. "Control of hydraulic wind power transfer system under wind and load disturbances," *IEEE Trans. Ind. Appl.*, vol. 54, no. 4, pp. 3596-3603, Aug. 2018, 10.1109/TIA.2018.2813970.

[19] X. D. Kong, C. Ai and J. Wang, "A summary on the control system of hydrostatic drive train for wind turbines," *Chin. Hydraul. & Pneumatics*, n. 1, pp.1-7, Jan. 2013.

[20] J. Li and W. Yuan, "Design and numerical simulation of a counter-rotating wind turbine," *Fluid Mach.*, vol. 41, no. 5, pp. 22-28. Feb. 2013, 10.3969/j.issn.1005-0329.2013.05.006.

[21] Z. H. Jiang and X.W. Yu, "Modeling and control of an integrated wind power generation and energy storage system," in *Proc. Power Energy Soc. General Meeting*, Calgary, Alberta, Canada, 2009, pp. 1-8.

[22] C. Ai, L. J. Chen, X. D. Kong, et al, "Characteristics simulation for hydraulic wind turbine," *China Mach. Eng.*, vol.26, no. 11, pp. 1527-1531. Jun. 2015, 10.3969/j.issn.1004-132X.2015.11.017.

[23] J. H. Wang. Advanced Nonlinear Control Theory and Its

Application [M]. Beijing: Beijing Science Press: 2012, 8-55.

[24] Sreenath K, Park H W, Poulakakis I, et al, "A compliant hybrid zero dynamics controller for stable, efficient and fast bipedal walking on MABEL," *Int. J. Rob. Res.*, vol. 30, no. 9, pp. 1170-1193, Sept. 2011, 10.1177/0278364910379882.

[25] S. Bharadwaj, A. V. RAO and D. M. Kenneth., "Entry trajectory tracking law via feed-back linearization," *J. Guid. Control Dyn.*, vol. 21, no. 5, pp. 726-732, Oct. 1998, 10.2514/2.4318.

Chao Ai was born in Tangshan, Hebei, China in 1982. He received the B.S. degrees in mechanical engineering and automation from Yanshan University, Qinhuangdao, China, in 2005, and the M.S. and Ph.D. degrees in fluid power transmission & control from Yanshan University, Qinhuangdao, China, in 2008 and 2013, respectively.

He has been working in Yanshan University since 2013. From 2013 to 2015, he was a Lecturer in Yanshan University. He is currently an Associate Professor, Master's Supervisor and Doctoral Supervisor in Yanshan University, Qinhuangdao, China. His current research interests include fluid power transmission and control, intelligent hydraulic wind power, fluid vibration and suppression, electro-hydraulic servo system and the optimum design of hydraulic components.

He was a recipient of the top-notch young talents in Hebei Province, the first prize of China Machinery Industry Science and Technology Award, the first prize of Hebei Science and Technology Progress Award, the first prize of Tianjin Science and Technology Progress Award, and the title of "cutting-edge engineering" talent in Yanshan University.

Wei Gao was born in Qinhuangdao, Hebei, China in 1990. He received the B.S. degrees in measurement and control technology and instruments from Yanshan University, Qinhuangdao, China, in 2014, and the M.S. degrees in detection technology and automation device from Yanshan University, Qinhuangdao, China, in 2017.

He is currently a doctoral candidate with Yanshan University, Qinhuangdao, China. His current research interests are intelligent hydraulic wind power and electro-hydraulic servo system.

Lijuan Chen was born in Chengde, Hebei, China in 1989. She received the B.S. degrees in mechanical engineering and automation from Yanshan University, Qinhuangdao, China, in 2014, and the M.S. degrees in mechanical and electronic engineering from Yanshan University, Qinhuangdao, China, in 2017.

She has been working in Nanjing Institute of Technology since 2018. She is currently an assistant experimentalist in Nanjing Institute of Technology, Nanjing, China. Her current research interests are intelligent hydraulic wind power, electro-hydraulic servo system and fault diagnosis of hydraulic valve.

Jiawei Guo was born in Shijiazhuang, Hebei, China in 1995. He received the B.S. degrees in mechanical engineering and automation from Yanshan University, Qinhuangdao, China, in 2018.

He is currently a master degree candidate with Yanshan University, Qinhuangdao, China. His current research interest is intelligent hydraulic wind turbine.

Xiangdong Kong was born in Qiqihaer, Heilongjiang, China in 1959. He received the B.S. degrees in mechanical engineering from Zhejiang University, Hangzhou, China, in 1982, the M.S. degrees in fluid power transmission & control from Northeast Heavy Machinery College, Qiqihaer, China, in 1985, and the Ph.D. degrees in fluid power transmission & control from Yanshan University, Qinhuangdao, China, in 1991.

Since 1991, He has been working in Yanshan University, Qinhuangdao, China. From 1991 to 1994, he was the Lecturer and Associate Professor in Yanshan University. From 1994 to 1996, he was the Deputy Director of the Department of Mechanical and Electrical Control Engineering in Yanshan University. From 1996 to 1997, he was the Director of the President Office in Yanshan University. Since 1996, he has been the Professor of Yanshan University. From 1997 to 2003, he was the Dean of the School of Mechanical Engineering in Yanshan University. Since 2003, he has been the Vice President and the Doctoral Supervisor of Yanshan

University. His current research interests include fluid power transmission and control, intelligent hydraulic wind power, the fluid vibration and suppression, electro-hydraulic servo system, the optimum design of hydraulic components and the theory and control of conveyor turbine.

Andrew Plummer received the B.Eng. degree from the University of Bath, England, in1987, and the Ph.D. degree from the same university in 1990.

From 1990 to 1993 he worked as a Research Engineer for Rediffusion Simulation. From 1994 to 1999, he was a Lecturer at the University of Leeds. From 1999 to 2006 he was the global control systems R&D manager for Instron. Since 2006 he has been Professor of Machine Systems and Director of the Centre for Power Transmission and Motion Control in the University of Bath.

His research interests are in motion and force control, particularly for servo hydraulic systems. Recent research projects have concerned hybrid hydraulic/piezoelectric actuation, robotic powered prostheses, additively manufactured hydraulic components, and fluid-actuation integrated into tensegrity structures. Professor Plummer is Chairman of the Global Fluid Power Society.